2024 IEEE International Conference on Robotics and Automation (ICRA 2024)
May 13-17, 2024. Yokohama, Japan

Soft Hand Extension Glove with Thumb Abduction and Extension Assistance

Disheng Xie[1], Yujie Su[1], Xiangqian Shi[1], Zheng Li[2] and Raymond Kai-yu Tong[1]

***Abstract*— Hand extension is crucial for stroke survivors with spasticity, where their fingers become rigid and their thumb remains curled within the palm. Due to the underactuated nature of the hand, the dominance of flexor muscles over extensors, and the limited surface area available, developing an extension glove with thumb assistance poses a challenge for researchers. This paper introduces a fully wearable soft hand extension glove based on the X-pouch and strap system, addressing the above challenges. The glove enables adequate finger extension, thumb abduction, and extension for high MAS score patients. Modelling and testing revealed extension torques of up to 2.7 Nm at the MCP joint and 0.67 Nm at the PIP and DIP joints. Performance evaluation, including comparison with existing methods, demonstrated the glove's superior extension capabilities using a model hand with realistic stiffness. Furthermore, the glove's effectiveness was confirmed through testing on a stroke patient with MAS = 2, validating its on-body functionality.**

I. INTRODUCTION

Hand dysfunction in stroke patients has a significant impact on their independence and daily activities [1]. Addressing the specific needs of stroke patients with spasticity is crucial, as this condition affects approximately 40% of stroke survivors [2], [3]. Spasticity, characterized by excessive muscle contractions, results in abnormal hand flexion and clenched fists. For them, hand extension assistance is more important than hand flexion. Hand exoskeletons have shown effectiveness in extending their hand and reducing spasticity, such as the Hand of Hope [4], KULEX-Hand [5] and Maestro-Hand [6], which have strong clinical evidence for rehabilitation [7]–[9]. However, the complex structures, high stiffness, and weight of exoskeletons hinder natural movement and limit their use in home-based settings [10].

Researchers have recognized the problems and create various gloves for assisting and rehabilitation training at home [11], [12]. In current literature, there exists mainly three types of gloves designed for hand rehabilitation with extension assistance. The first type utilizes a steel sheet or elastic force to passively extend the fingers [13]–[16]. This design is compact ascribing to the low profile of the sheet or elastic components. The second type utilizes a revert-bending fluid-driven method, such as the one-pouch method [17], [18] , several-module contact method [19], or negative-driven bellow method [20]. However, the torque-angle characteristics of the elastic materials or fluid structures used in the above extension mechanism present challenges in achieving sufficient backup torque in a compact manner,

Fig. 1. The overall design of the extension glove is depicted in the figure. The serial numbers, 1, 2, 3, etc., correspond to the straps that will be consistently referred to throughout the entire paper. (a) Perspective view: The glove features an adjustable belt system that can accommodate users with different hand sizes. Its one-sided wearing design allows for convenient and quick application and removal, particularly beneficial for spastic hands. (b) Back of hand side view: Each MCP joint is connected to strap 1 and X-pouches for extension, whereas the PIP and DIP joints share strap 2 and a corresponding X-pouch for extension. (c) Palm side view: Strap 4 and an X-pouch are positioned on the thenar to facilitate abduction of the CMC joint. (d) Thumb side view: Strap 5 and an X-pouch are utilized to extend the IP joint, while the MCP and CMC joints share strap 3 and an X-pouch for extension.

This work was supported by the Research Grants Council of Hong Kong (GRF 14216622). Corresponding author: Raymond Kai-yu Tong and Zheng Li.

[1]Disheng Xie, Yujie Su, Xiangqian Shi and Raymond Tong are with the Department of Biomedical Engineering, the Chinese University of Hong Kong, Hong Kong SAR, China kytong@cuhk.edu.hk

[2]Zheng Li is with the Department of Surgery, the Chinese University of Hong Kong, Hong Kong SAR, China lizheng@cuhk.edu.hk

This work involved human subjects. Approval of all ethical and experimental procedures and protocols was granted by the Joint Chinese University of Hong Kong-New Territories East Cluster (CUHK-NTEC) Clinical Research Ethics Committee under granted number NCT03286309.

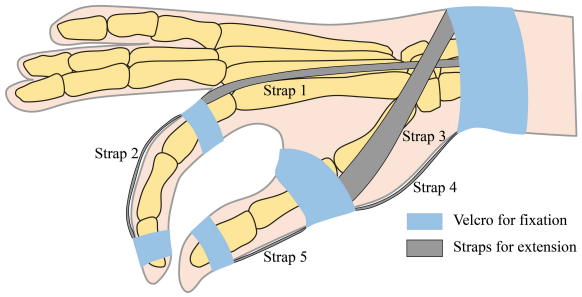

Fig. 2. The glove features a strap configuration for effective extension of each fingers. The straps are securely attached to the respective joints using Velcro for fixation. To account for the underactuation of the fingers, a dual-strap system is employed to extend each finger, preventing unnatural angles. Strap 1 is specifically designed for extending the MCP joint. Strap 2 is utilized to extend both the PIP and DIP joints when lifted away from the fingers. Strap 3 contributes to the extension of both the MCP and CMC joints. Strap 4 is responsible for the abduction of the CMC joint. Strap 5 is dedicated to extending the IP joint.

thereby limiting the effective extension of the fingers.

The third type is the cable-driven method [21]–[26], which is widely used in various types of assisting gloves. However, the cable-finger system is an under-actuated system, and when the fingertips are pulled, it may cause unnatural angles between the metacarpophalangeal (MCP), proximal interphalangeal (PIP), and distal interphalangeal (DIP) joints. Additionally, when the fingers are flexed around 180 degrees, the cables can cause stress concentration or parasitic forces on the PIP and DIP joints, leading to pain and discomfort [27]. In some previous designs [22], the DIP joint is fixed to mitigate the discomfort around that joint, but this approach affects the natural movement of the fingers.

Furthermore, most existing hand gloves fail to provide adequate assistance for thumb movement, despite the fact that the thumb's motion is essential for nearly half of daily tasks [28], [29]. Stroke survivors with spasticity often experience thumb flexed into the palm [30]. Accommodating the underactuated structure, the sum of physical cross-section area of thumb flexors is much larger than extensors [31] and the scarcity of surface area around the thumb, achieving abduction and extension of the thumb poses a significant challenge. Researchers have explored various methods to provide thumb assistance, including the application of cable-driven mechanisms [14], [23]. However, it is more common to immobilize the thumb using a splint in a fixed position [32], [33]. This approach, while providing stability, limits the glove's ability to support complex daily tasks [34]. Some soft gloves have achieved thumb abduction to simplify the system design [18], [26], [35]. However, if only abduction is assisted, tasks such as pinching may still be challenging.

Therefore, there is a need for an effective hand extension glove that provides both thumb abduction and extension assistance. To address these considerations, the design concept of the glove incorporates the observation of a one-pouch type mechanism, which can be abstracted as a strap with fixed ends on the fingers and an inflation pouch represented by a force acting on the strap. The low backup torque is caused by the limited inflation of the conventional pouch causing reduced force on a strap when the extension angle increases. Therefore, a method that reduces force reduction with inflation is required. This paper introduces an improvement method based on the previous design using special designed strap systems and X-pouch showing more promising results on dealing the above considerations.

II. Concept and Design

A. Hand Extension Glove Base Design

As mentioned earlier, the glove is based on strap systems where two ends are fixed on the joints to be assisted. To achieve adequate finger extension without causing discomfort or unnatural angles, a different approach is taken. Instead of fixing one end at the fingertip and the other end at the wrist, two separate straps are used to extend the PIP-DIP joints and the MCP joint, as shown in Fig. 1 and Fig. 2. In this configuration, one end of strap 1 is fixed on the wrist, while the other end is fixed on the proximal phalanx. Similarly, one end of strap 2 is fixed on the proximal phalanx, and the other end is fixed on the distal phalanx.

For thumb assistance, at least three straps are required to achieve extension and abduction of the IP joint, extension of the MCP joint, and extension of the CMC joint, as shown

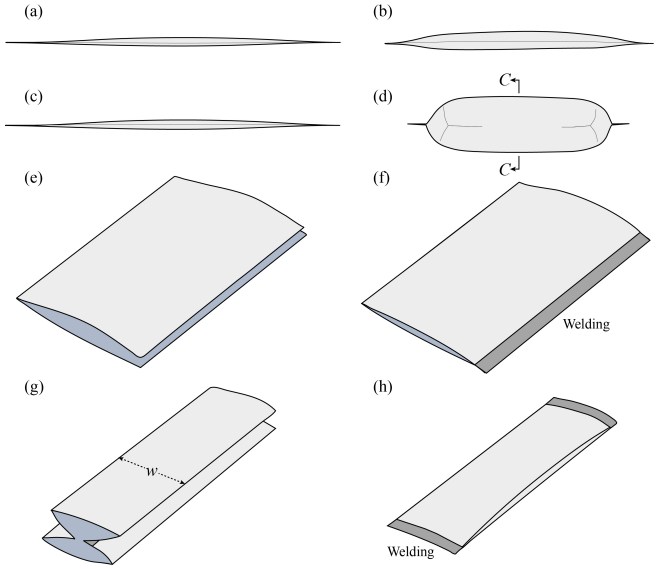

Fig. 3. The comparison of conventional pouch and X-pouch, along with the manufacturing method of X-pouch. (a) The side view of the deflated conventional pouch is shown, which has a standard thickness. (b) The side view illustrates the inflated conventional pouch, demonstrating its expanded shape when air or fluid is introduced. (c) The side view showcases the deflated X-pouch, which possesses a comparable thickness to the conventional pouch. (d) The side view displays the inflated X-pouch, emphasizing its significant increase in height compared to the conventional pouch. As a result, the X-pouch exhibits a slower decrease in output force in the vertical direction, indicating a higher backup force. The sectional shape at C-C corresponds to Fig. 4(d). (e) A single piece of the TPU membrane is folded, preparing it for the subsequent steps. (f) One side of the membrane is welded together to create a sealed edge. (g) The left and right edges of the membrane are folded inward, forming an X-shaped section. (h) The upper and lower ends of the folded membrane are welded together, completing the X-pouch structure.

in Fig. 1 and Fig. 2. One end of strap 3 and strap 4 is fixed on the proximal phalanx, while the other end is fixed on the wrist. One end of strap 5 is fixed on the proximal phalanx, and the other end is fixed on the distal phalanx.

B. High Backup Torque Pouch Design

In a fluid-driven structure, the output force becomes zero when the structure is fully inflated, regardless of the initial force generated. This means that the backup torque is zero when the entire stroke is used for actuation. To achieve higher backup torques, it is necessary to slowly decrease the force F with height or expansion, ensuring that not all of the stroke is utilized for actuation.

Conventional pouch designs, such as the one described in [36], exhibit a fast decrease in generated force F during inflation. Additionally, the limited inflation of the pouches as shown in Fig. 3(a-b) often fail to fully fill the gaps between the strap and the finger. Therefore, the fundamental requirement for an effective design is to achieve a sufficient expansion ratio.

To address these issues, a new type of pouch called the X-pouch is introduced, as illustrated in Fig. 3(c-d). The X-pouch is constructed by folding a TPU membrane into two accordion folds and welding the two ends together. as shown in Fig. 3(e-h). When the X-pouch is inflated, it naturally takes on a cuboid shape, lifting the strap and extending the fingers. The height increase achieved with the X-pouch is larger than required and significantly greater than that of conventional pouches, as shown in Fig. 3(a-b). This design results in a structure with higher backup forces. Furthermore, the inflated cuboid shape of the X-pouch provides stability on the fingers despite its narrow width.

By placing the X-pouches under the straps in the appropriate locations, the straps are lifted, and the fingers are extended, completing the assembly of the glove as shown in Fig. 1. It is important to note that the X-pouches used for the fingers have a width of 15 mm, while the X-pouches for other joints have a width of 30 mm. The length of the X-pouches varies depending on the specific joint being assisted.

III. Modelling

To analyze of the complex X-pouch-strap 1-fingers system associated with the MCP joint, the virtual work principle is employed as a modeling method with necessary simplification. The approach is as follows:

$$P \cdot dV = M \cdot d\alpha \tag{1}$$

where α represent the angle between the second metacarpal l_1 and the proximal phalanges l_2, as depicted in Fig. 4(a). In this figure, M denotes the assistance torque acting on the MCP joint, while P and V represent the pressure and volume of the X-pouch (light gray), respectively. To establish the relationship between the torque M and the angle α, it is necessary to model the volume changes of the X-pouch, assuming a constant pressure P. Additionally, t denotes the half thickness of the second metacarpal and the proximal phalanges, as illustrated in Fig. 4(a).

As shown in Fig. 4(a-b), the inflation of the X-pouch and the height h cause the MCP joint to extend through strap 1 (l_3, l_4, and l_5). Through observations, it can be noted that l_4+

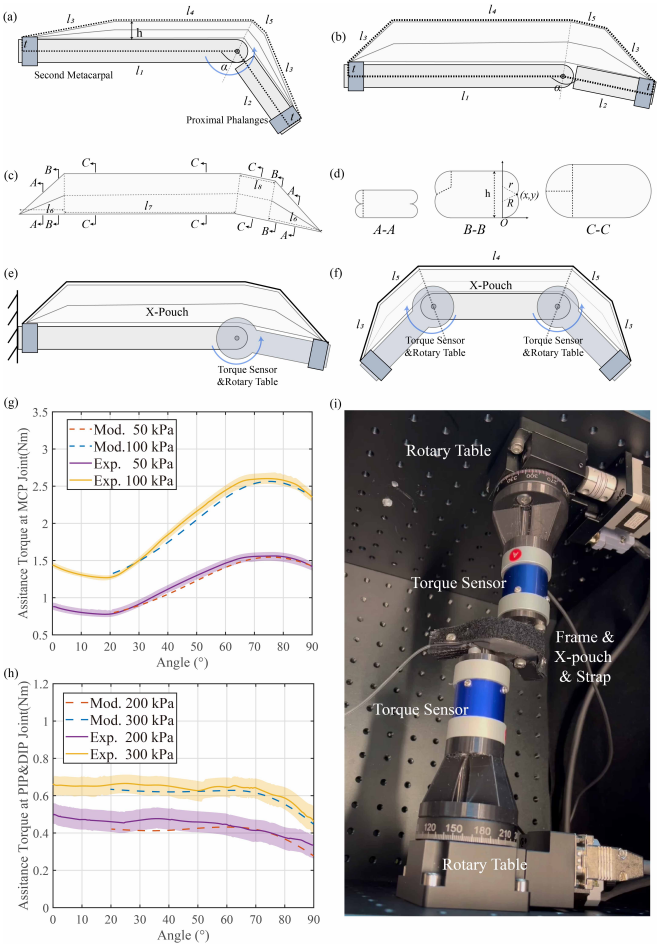

Fig. 4. Extension Mechanism Model, Test Bench Setup, and Results: (a) A model is constructed to represent the Strap 1-X-Pouch-Second Metacarpal-Proximal Phalanges system. In this model, the X-pouch inflates to drive the MCP joint to extend. (b) The X-pouch continues to inflate, pushing Strap 1 upward and driving the MCP joint to further extend. (c) The state of inflation of the X-pouch positioned under Strap 1 is depicted, showing the shape of inflation necessary for extending the MCP joint now. (d) The sectional shape of the X-pouch at different heights is illustrated, indicating how the shape changes during inflation. (e) A test setup is designed to measure the assistance torque applied to the MCP joint. The setup consists of two connected links, with one fixed to a base and the other connected to a torque sensor driven by a rotary table. Strap 1 and the X-pouch are connected to the ends of the links, and the torque is recorded when the X-pouch is inflated, and the link rotates. (f) Another test setup is employed to measure the assistance torque on the PIP and DIP joints. The setup includes side links connected to torque sensors, driven by opposed rotary tables to rotate the links in opposite directions. Strap 2, fixed on both sides, is pushed by the inflated X-pouch, and the assistance torque on the PIP and DIP joints is recorded. (g) The experimental extension torque at the MCP joint is plotted against the extended angle. The results indicate a trend of initially decreasing, then increasing, and finally decreasing torque at the last part. The model accurately fits the tested results, except for the first 20 degrees of extension. (h) The experimental torque on the PIP and DIP joints is plotted against the extended angle. The results show a quasi-stable torque across most of the range, with a decrease observed at the last part of the extension. Similarly, the model results align well with the experimental data. (i) A photograph of the dual-motor assistance torque test bench is provided.

l_5 increases with the height h. Assuming a linear relationship that

$$l_4 + l_5 = kh \tag{2}$$

where the coefficient k represents the rate at which $l_4 + l_5$ increases with the height h. Initially, k can be determined through measurements and subsequently adjusted to obtain the best fitting result. The bisector of the angle between l_4 and l_5 aligns with the bisector of α. By considering the given limiting conditions, all the parameters can be calculated as functions of h based on the geometric constraints. For instance, $\theta = f_1(h)$ and $l = f_2(h)$. The detailed but trivial calculation process is omitted here due to space limitations. It is important to note that l_6, l_7, and l_8 should also be determined as functions of h since they are required for subsequent steps. The modeling methodology for Strap 2, PIP, and DIP joints follows a similar approach. The key difference is that Strap 2 is divided into five symmetrical parts: l_3, l_5, l_4, l_5, and l_3, as shown in Fig. 4(f), and their lengths satisfy the relationship $l_4 + 2l_5 = kh$.

Once the length of the outer strap is determined, the next step is to use these parameters to calculate the volume V of the X-pouch. The inflation of the X-pouch follows the process depicted in Fig. 4(a-b). Figure 4(c) represents the X-pouch under Strap 1 in Fig. 4(b), and the sectional shape at different heights is shown in Fig. 4(d). For example, at a lower height (A-A), the arcs on both sides are compressed, resulting in two exposed arcs with a central angle of 180°. As the height h increases, such as at height (B-B), the compressed part decreases, and the central angle of the arcs becomes less than 180°. When the X-pouch is fully inflated, as shown in Fig. 4(c) (C-C), the central angle of the two arcs reduces to 90°. Therefore, the sectional area S is a function of the height h. As the X-pouch continues to inflate, h increases, and the sectional shape mode remains the same. The section under l_4 and l_5 always maintains the C-C state because this part is less constrained by the boundaries on both sides, only the sectional area changes with h as observed in Video 1 and Fig. 4(i). It is worth noting that the upper bound of the h equals to $h_u = 2w/\pi$ where w is the width of the X-pouch as shown in Fig. 3(g). By establishing the coordinate system as shown in Fig. 4(d), assuming the coordinates of the intersecting point of the two arcs are (x, y), the radii of the two arcs, denoted as r and R, can be calculated using the following equations:

$$x^2 + (y - R)^2 = R^2 \tag{3}$$

$$x^2 + [y - (h - r)]^2 = r^2 \tag{4}$$

Where $y = 0.4h$ as observed and x increases from 0 to the coordinate of the corresponding point at C-C state.

Then the sectional area S and the center angle of the arc can be obtained after obtaining the radii of the arcs as functions of the height $S = f(h)$. Because the X-pouch has an irregular shape, the volume of the X-pouch cannot be directly calculated using a simple equation. Instead, numerical algorithms is employed to estimate the volume as follows:

$$V = \int_0^{2l_6+l_7+l_8} S\,(h)\,dl \tag{5}$$

By combining Equation 1 and 5, the relationship between the assistance torque M and the angle θ can be established when traversing h from 0 to h_u, as illustrated in Fig. 4(g). It can be observed that when the pressure P remains constant, the torque M initially increases with the angle θ, reaching a peak value, and then decreases for angles larger than 75°. It is important to note that the model accurately depicts the phenomenon after 20°, as the inflation of the X-pouch in the initial 20° involves more complex processes that are difficult to describe. Similarly to the approach used to obtain the simulated torque at the MCP joint, the modelled result of the assistance torque is presented in Fig. 4(h). The result illustrates an initial quasi-static phase followed by a decrease in torque.

IV. Experiment

A. Bench test

To test the extension torque on MCP joint, a frame with a sectional view identical to Fig. 4(b) was constructed as shown in Fig. 4(e), and the side link was connected to a torque sensor driven by a rotary table. When the rotary table drives the link to rotate at a constant speed and the inner pressure keeps the same, torque sensor record the corresponding torque. The test was repeated three times, and the testing results are presented in Fig. 4(g), indicating a maximum torque of 2.7 Nm near the final state. When the frame is fully extended, the torque is 2.4 Nm at 100 kPa, demonstrating sufficient backup torque for the extension of the MCP joint. This behavior relatively aligns with the natural increasing relationship between passive extension torque of fingers and angle, as described in the study by Kamper [37]. The experimental result shows the accuracy of the model. Due to the wider X-pouch used in this experiment, the expansion ratio of the pouch is much larger than required. Consequently, the pull-up effect of inflation causes the output torque continue to increase in the second half of the stroke. Moreover, since the sectional area of the X-pouch in this experiment is larger, the maximum pressure requirement is reduced.

To test the extension torque on PIP and DIP joints, a dual motor-driven test bench was constructed, as illustrated in Fig. 4(f) and Fig. 4(i). The test bench consists of a 3-links frame, representing the proximal phalanges, intermediate phalanges, and distal phalanges. The two side links are driven by the same rotary table and rotate in opposite directions. X-pouch with a width of 15 mm are attached to the link when the links are vertically aligned. Subsequently, the X-pouch is pressurized at 200 kPa and 300 kPa, and the rotary tables drive the side links to extend from a fully flexed state to a fully extended state, simulating the extension of the PIP and

Fig. 5. Model Test of the Hand Extension Glove: (a) The model hand is equipped with 16 degrees of freedom. The joints of the index finger and thumb finger are reinforced with torsion springs to replicate the behavior of stroke survivors with spasticity. (b) The index finger is fitted with strap 1 and strap 2, while the X-pouch is in its initial state. (c) The X-pouch positioned under strap 2 is inflated, resulting in the extension of the PIP and DIP joints of the index finger. (d) The X-pouch located under strap 1 is inflated, facilitating the extension of the MCP joint of the index finger. (e) Extension effect using a passive extension method is demonstrated on the model hand [13]. (f) Cable-driven extension is employed to extend the model hand [21]. (g) The hand extension is achieved using a method involving a single pouch [17]. (h) The model hand is extended through a method utilizing negative pressure-driven bellows [20]. (i) The thumb is equipped with strap 3 and strap 4, while the X-pouch is in its initial state. (j) The X-pouch positioned under strap 4 is initially inflated, leading to the abduction of the CMC joint of the thumb. (k-l) Subsequently, the X-pouch under strap 3 is inflated, extending the CMC joint of the thumb. (m) The thumb is equipped with strap 3, strap 4, and strap 5 while the X-pouch is in its initial state. (n) The X-pouch located under strap 3 is inflated, resulting in the extension of the CMC joint of the thumb. (o) Next, the X-pouch under strap 5 is inflated, extending the IP joint of the thumb. (p) Finally, the X-pouch under strap 4 is inflated, facilitating the abduction of the CMC joint of the thumb.

DIP joints. The extension torque is measured three times, and the testing results are presented in Fig. 4(h).

The test results indicate that the maximum torque is 0.67 Nm at 300 kPa in the fully flexed state, and even in the fully extended state, there is still a residual backup torque of 0.42 Nm. The torque initially keeps quasi-staic but then decreases in the second half of the stroke due to the end of the inflation of the X-pouch, as depicted in Fig. 4(h). This verifies the torque pulling up effect of the model otherwise the output torque reduces with the expansion causing low backup torque.

B. Model test

Before conducting tests on real hands, a model hand was developed to simulate the behavior of stroke survivors with spasticity, as depicted in Fig. 5(a). The model hand includes 16 degrees of freedom (DOFs), particularly focusing on the DOFs around the thumb to achieve palmar abduction, radial abduction, and extension. The joint stiffness is implemented using torsion springs aligned with the joints. Torsion springs adequately represent the behavior of spastic fingers, as previous studies have shown that the relationship between torque and angle is nearly linear in such cases [37], [38]. The torsion spring used in the model hand starts at a 90° initial state and requires approximately 0.35 Nm of torque when rotated about 180°, as measured by a torque wrench. Thus, the model hand effectively simulates spasticity with a Modified Ashworth Scale (MAS) score of 2 [39], [40].

Next, the extension mechanism proposed in the paper was applied to the fingers of the model hand, and its effectiveness was compared with other published methods, as shown in Fig. 5(b-d), demonstrating how the X-pouches first drive the distal DIP and PIP joints to extend, followed by the MCP joint, resulting in adequate extension. This illustrates the effectiveness of the mechanism. Fig. 5(e) shows the passive method driven by a steel sheet, which achieves a maximum opening angle of approximately 90° under these conditions, similar to the result obtained using the one-pouch method shown in Fig. 5(g). The negative-pressure-driven bellow method performs the worst, with minimal finger extension. Although the cable-driven method can extend the fingers to extended state, the PIP joint exhibits hyper extension as the cables are pulled, posing a potential danger in this mechanism.

The assistance around the thumb was also tested. As depicted in Fig. 5(i-j), the X-pouch under strap 4 is first inflated, resulting in CMC abduction only. Then, as shown in Fig. 5(k-l), the X-pouch under strap 3 is inflated, resulting in additional MCP and CMC joint extension. Different inflation sequences were also tested to examine whether the two straps affect each other. As shown in Fig. 5(m-n), the X-pouch under strap 3 is first inflated, followed by MCP and CMC joint extension. Then, as displayed in Fig. 5(n-o), the X-pouch under strap 5 is inflated, causing IP joint extension. Finally, in Fig. 5(o-p), the X-pouch under strap 4 is inflated, resulting in additional radial abduction. This demonstrates that the two DOFs do not significantly affect each other.

C. Subject test

A single chronic stroke patient with a MAS score of 2 was recruited to assess the effectiveness of the hand extension glove. The patient initially had an index finger resting angle

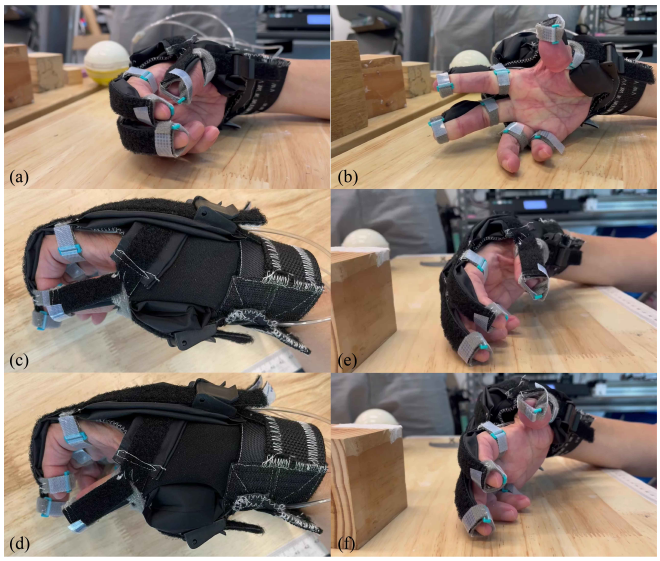

Fig. 6. Subject test. (a) The subject with MAS score = 2 wears the hand extension glove. (b) Extension effect on the patient's hand. (c-d) CMC joint abduction test result (e-f) MCP and CMC joints extension result.

of approximately 99°, with the thumb curled into the palm. The grasping performance was evaluated using the standard test procedure of the Action Research Arm Test (ARAT) [41]. With the patient's active force alone, only a 2.5 cm block could be grasped. However, with the assistance of the unaffected hand, the patient was able to grasp a 5 cm block, as demonstrated in Video 1.

The effectiveness of the one-pouch configuration was then tested. In Fig. 6(a-b), the assistance effect on the extension of the index and middle fingers was examined. Similar to the model test shown in Fig. 5(b-c), the PIP and DIP joints were extended first, mimicking the function of the lumbrical muscle, followed by extension of the MCP joint. The assistance torque provided by the X-pouch under strap 2 was lower than that of the X-pouch under strap 1. The inflation sequence was found to be more suitable for the extension mechanism because, assuming that the total length of the muscles and tendons that flex the finger remains fixed, extending the PIP and DIP joints requires less torque, while extending the MCP joint requires more torque. The index and middle fingers were extended without causing pain or discomfort, as reported by the patient.

As shown in Fig. 6(e-f), by pressurizing the X-pouch under strap 3, the MCP and CMC joints of the thumb were extended from the patient's resting angle to the extended state, demonstrating the functionality of the mechanism around these two joints. In Fig. 6(c-d), pressurizing the X-pouch under strap 4 caused abduction of the CMC joint with an angle of 23°, which is less than the maximum passive extension range. This deviation in the abduction effect was due to the strap fixed on the patient's wrist being too wide, covering the CMC joint and affecting the abduction effect. This result emphasizes the importance of individualized design and highlights the plan to utilize customized parameter in the next version of the glove design to ensure a precise fit and optimal anchoring position. Finally, the ability to open the entire hand was tested, as shown in Fig. 6(a-b). With the assistance of the glove, the patient was able to lift a 7.5 cm block, as demonstrated in Video 1.

V. CONCLUSIONS AND DISCUSSION

This study introduces a soft hand extension glove that incorporates thumb abduction and extension assistance using strap system and X-pouches with a high expansion ratio. The extension mechanism, which can be applied to extend both fingers and the thumb, achieves a high backup torque to facilitate adequate extension. The mathematical model provides an explanation for the high backup torque mechanism. The assisting torque was also tested using a single and dual motor-driven test bench, revealing up to 0.67 Nm for extending the PIP and DIP joints and 2.7 Nm for extending the MCP joints.

Subsequently, a comparison was made with other published extension mechanisms on a model hand. The mechanism shows high backup extension torque over passive-driven method and one-pouch-driven method, avoids unnatural finger angles over cable-driven method and shows larger extension ability over negative pressure-driven bellow because the higher-pressure difference of the positive pressure. Finally, the adequate extension effect is verified on a stroke patient with MAS score equals 2.

Although we have conducted preliminary tests on a patient to evaluate the effectiveness of the glove, further studies involving a larger sample size are necessary to verify its rehabilitation effect during home training or daily life activities. Additionally, the experiment highlighted the significance of cooperative control of air pressure in implementing task-oriented rehabilitation training. This aspect will be the focus of our next research phase, aiming to enhance the functionality and practicality of the glove for effective rehabilitation training.

Furthermore, while the current focus has been on hand extension, we have observed that the extension mechanism has the potential to be extended to other joints, such as the wrist and elbow. Stroke patients often experience abnormal synergy not only in their hands but also in other affected areas. Therefore, in future studies, we plan to integrate the extension mechanism for the hand, wrist, and elbow, enabling comprehensive rehabilitation training that addresses abnormal synergies across multiple joints.

REFERENCES

[1] F. J. Carod-Artal, D. Stieven Trizotto, L. Ferreira Coral, and C. Menezes Moreira, "Determinants of quality of life in Brazilian stroke survivors," *Journal of the Neurological Sciences*, vol. 284, no. 1-2, pp. 63–68, Sept. 2009.

[2] G. E. Francisco and J. R. McGuire, "Poststroke Spasticity Management," *Stroke*, vol. 43, no. 11, pp. 3132–3136, Nov. 2012.

[3] F. C. Huang and J. L. Patton, "Movement distributions of stroke survivors exhibit distinct patterns that evolve with training," *Journal of NeuroEngineering and Rehabilitation*, vol. 13, no. 1, p. 23, Dec. 2016.

[4] N. Ho, K. Tong, X. Hu, K. Fung, X. Wei, W. Rong, and E. Susanto, "An emg-driven exoskeleton hand robotic training device on chronic stroke subjects: task training system for stroke rehabilitation," in *2011 IEEE international conference on rehabilitation robotics*. IEEE, 2011, pp. 1–5.

[5] M. B. Hong, S. J. Kim, Y. S. Ihn, G.-C. Jeong, and K. Kim, "Kulex-hand: An underactuated wearable hand for grasping power assistance," *IEEE Transactions on Robotics*, vol. 35, no. 2, pp. 420–432, 2018.

[6] Y. Yun, S. Dancausse, P. Esmatloo, A. Serrato, C. A. Merring, and A. D. Deshpande, "An emg-driven assistive hand exoskeleton for spinal cord injury patients: Maestro," in *IEEE International Conference on Robotics and Automation (ICRA)*, 2017.

[7] X. Hu, K. Tong, X. Wei, W. Rong, E. Susanto, and S. Ho, "The effects of post-stroke upper-limb training with an electromyography (emg)-driven hand robot," *Journal of Electromyography and Kinesiology*, vol. 23, no. 5, pp. 1065–1074, 2013.

[8] E. A. Susanto, R. K. Tong, C. Ockenfeld, and N. S. Ho, "Efficacy of robot-assisted fingers training in chronic stroke survivors: a pilot randomized-controlled trial," *Journal of neuroengineering and rehabilitation*, vol. 12, pp. 1–9, 2015.

[9] W. Rong, K. Y. Tong, X. L. Hu, and S. K. Ho, "Effects of electromyography-driven robot-aided hand training with neuromuscular electrical stimulation on hand control performance after chronic stroke," *Disability and Rehabilitation: Assistive Technology*, vol. 10, no. 2, pp. 149–159, 2015.

[10] D. Popov, I. Gaponov, and J.-H. Ryu, "Portable exoskeleton glove with soft structure for hand assistance in activities of daily living," *IEEE/ASME Transactions on Mechatronics*, vol. 22, no. 2, pp. 865–875, 2016.

[11] V. Sanchez, C. J. Walsh, and R. J. Wood, "Textile Technology for Soft Robotic and Autonomous Garments," *Advanced Functional Materials*, vol. 31, no. 6, p. 2008278, Feb. 2021.

[12] C.-Y. Chu and R. M. Patterson, "Soft robotic devices for hand rehabilitation and assistance: A narrative review," *Journal of Neuro-Engineering and Rehabilitation*, vol. 15, no. 1, p. 9, Dec. 2018.

[13] K. H. Heung, R. K. Tong, A. T. Lau, and Z. Li, "Robotic glove with soft-elastic composite actuators for assisting activities of daily living," *Soft robotics*, vol. 6, no. 2, pp. 289–304, 2019.

[14] D. H. Kim, Y. Lee, and H.-S. Park, "Bioinspired high-degrees of freedom soft robotic glove for restoring versatile and comfortable manipulation," *Soft Robotics*, vol. 9, no. 4, pp. 734–744, 2022.

[15] L. Cappello, K. C. Galloway, S. Sanan, D. A. Wagner, R. Granberry, S. Engelhardt, F. L. Haufe, J. D. Peisner, and C. J. Walsh, "Exploiting textile mechanical anisotropy for fabric-based pneumatic actuators," *Soft robotics*, vol. 5, no. 5, pp. 662–674, 2018.

[16] P. Polygerinos, Z. Wang, K. C. Galloway, R. J. Wood, and C. J. Walsh, "Soft robotic glove for combined assistance and at-home rehabilitation," *Robotics and Autonomous Systems*, vol. 73, pp. 135–143, 2015.

[17] H. K. Yap, P. M. Khin, T. H. Koh, Y. Sun, X. Liang, J. H. Lim, and C.-H. Yeow, "A fully fabric-based bidirectional soft robotic glove for assistance and rehabilitation of hand impaired patients," *IEEE Robotics and Automation Letters*, vol. 2, no. 3, pp. 1383–1390, 2017.

[18] L. Ge, F. Chen, D. Wang, Y. Zhang, D. Han, T. Wang, and G. Gu, "Design, modeling, and evaluation of fabric-based pneumatic actuators for soft wearable assistive gloves," *Soft robotics*, vol. 7, no. 5, pp. 583–596, 2020.

[19] B. W. Ang and C.-H. Yeow, "3d printed soft pneumatic actuators with intent sensing for hand rehabilitative exoskeletons," in *2019 International Conference on Robotics and Automation (ICRA)*. IEEE, 2019, pp. 841–846.

[20] D. Hu, J. Zhang, Y. Yang, Q. Li, D. Li, and J. Hong, "A novel soft robotic glove with positive-negative pneumatic actuator for hand rehabilitation," in *2020 IEEE/ASME International Conference on Advanced Intelligent Mechatronics (AIM)*. IEEE, 2020, pp. 1840–1847.

[21] A. Yurkewich, I. J. Kozak, D. Hebert, R. H. Wang, and A. Mihailidis, "Hand extension robot orthosis (hero) grip glove: enabling independence amongst persons with severe hand impairments after stroke," *Journal of neuroengineering and rehabilitation*, vol. 17, pp. 1–17, 2020.

[22] S. Park, M. Fraser, L. M. Weber, C. Meeker, L. Bishop, D. Geller, J. Stein, and M. Ciocarlie, "User-driven functional movement training with a wearable hand robot after stroke," *IEEE Transactions on Neural Systems and Rehabilitation Engineering*, vol. 28, no. 10, pp. 2265–2275, 2020.

[23] W. Chen, G. Li, N. Li, W. Wang, P. Yu, R. Wang, X. Xue, X. Zhao, and L. Liu, "Soft exoskeleton with fully actuated thumb movements for grasping assistance," *IEEE Transactions on Robotics*, vol. 38, no. 4, pp. 2194–2207, 2022.

[24] A. Yurkewich, I. J. Kozak, A. Ivanovic, D. Rossos, R. H. Wang, D. Hebert, and A. Mihailidis, "Myoelectric untethered robotic glove enhances hand function and performance on daily living tasks after stroke," *Journal of Rehabilitation and Assistive Technologies Engineering*, vol. 7, p. 2055668320964050, 2020.

[25] A. Yurkewich, D. Hebert, R. H. Wang, and A. Mihailidis, "Hand extension robot orthosis (hero) glove: development and testing with stroke survivors with severe hand impairment," *IEEE Transactions on Neural Systems and Rehabilitation Engineering*, vol. 27, no. 5, pp. 916–926, 2019.

[26] T. Bützer, O. Lambercy, J. Arata, and R. Gassert, "Fully wearable actuated soft exoskeleton for grasping assistance in everyday activities," *Soft robotics*, vol. 8, no. 2, pp. 128–143, 2021.

[27] K. Shi, A. Song, Y. Li, H. Li, D. Chen, and L. Zhu, "A cable-driven three-dof wrist rehabilitation exoskeleton with improved performance," *Frontiers in Neurorobotics*, vol. 15, p. 664062, 2021.

[28] J. N. Ingram, K. P. Körding, I. S. Howard, and D. M. Wolpert, "The statistics of natural hand movements," *Experimental brain research*, vol. 188, pp. 223–236, 2008.

[29] V. K. Nanayakkara, G. Cotugno, N. Vitzilaios, D. Venetsanos, T. Nanayakkara, and M. N. Sahinkaya, "The role of morphology of the thumb in anthropomorphic grasping: a review," *Frontiers in mechanical engineering*, vol. 3, p. 5, 2017.

[30] A. Thibaut, C. Chatelle, E. Ziegler, M.-A. Bruno, S. Laureys, and O. Gosseries, "Spasticity after stroke: physiology, assessment and treatment," *Brain injury*, vol. 27, no. 10, pp. 1093–1105, 2013.

[31] A. Cutts, R. Alexander, and R. F. Ker, "Ratios of cross-sectional areas of muscles and their tendons in a healthy human forearm." *Journal of Anatomy*, vol. 176, p. 133, 1991.

[32] K. H. L. Heung, Z. Q. Tang, L. Ho, M. Tung, Z. Li, and R. K. Y. Tong, "Design of a 3d printed soft robotic hand for stroke rehabilitation and daily activities assistance," in *2019 IEEE 16th International Conference on Rehabilitation Robotics (ICORR)*, 2019, pp. 65–70.

[33] X. Q. Shi, H. L. Heung, Z. Q. Tang, Z. Li, and K. Y. Tong, "Effects of a soft robotic hand for hand rehabilitation in chronic stroke survivors," *Journal of Stroke and Cerebrovascular Diseases*, vol. 30, no. 7, p. 105812, 2021.

[34] R. Parry, S. Macias Soria, P. Pradat-Diehl, V. Marchand-Pauvert, N. Jarrassé, and A. Roby-Brami, "Effects of hand configuration on the grasping, holding, and placement of an instrumented object in patients with hemiparesis," *Frontiers in neurology*, vol. 10, p. 240, 2019.

[35] Y. Wang, S. Kokubu, Z. Zhou, X. Guo, Y.-H. Hsueh, and W. Yu, "Designing soft pneumatic actuators for thumb movements," *IEEE Robotics and Automation Letters*, vol. 6, no. 4, pp. 8450–8457, 2021.

[36] R. Niiyama, X. Sun, C. Sung, B. An, D. Rus, and S. Kim, "Pouch Motors: Printable Soft Actuators Integrated with Computational Design," *Soft Robotics*, vol. 2, no. 2, pp. 59–70, June 2015.

[37] D. G. Kamper and W. Z. Rymer, "Quantitative features of the stretch response of extrinsic finger muscles in hemiparetic stroke," *Muscle & Nerve*, vol. 23, no. 6, pp. 954–961, June 2000.

[38] D. Kamper, R. Harvey, S. Suresh, and W. Rymer, "Relative contributions of neural mechanisms versus muscle mechanics in promoting finger extension deficits following stroke," *Muscle & Nerve*, vol. 28, no. 3, pp. 309–318, Sept. 2003.

[39] M. Blackburn, P. van Vliet, and S. P. Mockett, "Reliability of Measurements Obtained With the Modified Ashworth Scale in the Lower Extremities of People With Stroke," *Physical Therapy*, vol. 82, no. 1, pp. 25–34, Jan. 2002.

[40] J. Mehrholz, K. Wagner, D. Meißner, K. Grundmann, C. Zange, R. Koch, and M. Pohl, "Reliability of the Modified Tardieu Scale and the Modified Ashworth Scale in adult patients with severe brain injury: A comparison study," *Clinical Rehabilitation*, vol. 19, no. 7, pp. 751–759, Nov. 2005.

[41] T. Platz, C. Pinkowski, F. van Wijck, I.-H. Kim, P. Di Bella, and G. Johnson, "Reliability and validity of arm function assessment with standardized guidelines for the fugl-meyer test, action research arm test and box and block test: a multicentre study," *Clinical rehabilitation*, vol. 19, no. 4, pp. 404–411, 2005.